Journal of Photochemistry and Photobiology A: Chemistry 324 (2016) 184–191

Contents lists available at ScienceDirect

Journal of Photochemistry and Photobiology A: Chemistry

journal homepage: www.elsevier.com/locate/jphotochem

Electronic properties and photofragmentation mechanisms of pyrosulfuryl chloride, $ClSO_2OSO_2Cl$

Angélica Moreno Betancourt[a], Yanina B. Bava[a], Mauricio F. Erben[a], Reinaldo L. Cavasso Filho[b], Shengrui Tong[c], Maofa Ge[c], Carlos O. Della Védova[a], Rosana M. Romano[a,*]

[a] CEQUINOR (UNLP, CCT-CONICET La Plata), Departamento de Química, Facultad de Ciencias Exactas, Universidad Nacional de La Plata, Blvd. 120 N° 1465, CC 962, La Plata CP 1900, Argentina
[b] Universidade Federal do ABC, Av. dos Estados, 5001, CEP 09210-580 Santo André, São Paulo, Brazil
[c] State Key Laboratory for Structural Chemistry of Unstable and Stable Species, Beijing National Laboratory for Molecular Sciences (BNLMS), Institute of Chemistry, Chinese Academy of Sciences, Beijing 100190, People's Republic of China

ARTICLE INFO

Article history:
Received 17 February 2016
Received in revised form 14 March 2016
Accepted 24 March 2016
Available online 26 March 2016

Keywords:
Ionization potentials
Photochemistry
Coincidence techniques
Radicals
Synchrotron

ABSTRACT

The first ionization potential of $ClSO_2OSO_2Cl$, was determined by photoelectron spectroscopy at 12.25 eV. The photoelectron spectrum was interpreted, with the aid of DFT calculations, as composed by twelve ionizations of non-bonding electrons localized on the oxygen and chlorine atoms. Several resonant transitions of inner electrons to LUMOs were detected in the Total Ion Yield spectra taken with tuneable synchrotron radiation. Photofragmentation mechanisms of pyrosulfuryl chloride after single and double ionization were studied by means of coincidence techniques (PEPICO, Photoelectron-Photoion-Coincidence and PEPIPICO, Photoelectron-Photoion-Photoion-Coincidence). The main fragmentation mechanism in the valence energy region leads to the formation of $ClSO_2OSO_2^+$ fragment and a chlorine radical. Other fragments, like $ClSO_2^+$, SO_2^+, ClO^+ (arising from an atomic rearrangement) and SO_3^+ were observed to appear as the energy of the synchrotron light increases. The fragmentation channels after double ionization processes were inferred from the comparison of the shapes and experimental slopes of the coincidence islands for two ionic fragments originating from the same molecule in the PEPIPICO spectra, with the theoretical slopes calculated by the Eland's formalism. The mechanisms were independent of the incident radiation energy, revealing the lack of site-specific processes. All mechanisms were proposed to start from the rupture of either Cl–S or O–S single bonds for a species which comprises and originates a number of relevant environmental and atmospheric processes and photoevolutions.

1. Introduction

Pyrosulfuryl chloride, $ClSO_2OSO_2Cl$, and the hitherto unknown peroxide, $ClSO_2OOSO_2Cl$, were found as the main products of the photochemical gas-phase reaction between SO_2, O_2 and Cl_2 [1]. While $ClSO_2OSO_2Cl$ is thermally and photochemically (below 6 eV) stable, the peroxide has a half life time of 15 min in gas phase at low pressure, decomposing in SO_3 and Cl_2. The complete photochemical reaction, including the decomposition products, was interpreted as the catalytic oxidation of SO_2 to SO_3. It was proposed that this reaction could play an important role in atmospheric chemistry, particularly in regions of high Cl_2 and SO_2 abundances. It was also suggested that it could account for chemical processes responsible for the unexpectedly low oxygen content of the Venus stratosphere [2].

Although pyrosulfuryl chloride was a known substance since the beginning of the twenty century [3,4], there are no reports, as far as we know, on its photochemistry when exposed to ionizing radiation. The structural and conformational properties of this compound were also still unknown. In parallel to the work presented here, efforts to determine structural and conformational aspect of the title species are undertaken by our research group, using mainly FTIR matrix isolation spectroscopy at variable temperatures, gas electron diffraction analysis, and X-ray single crystal studies at low temperatures.

The study presented here is part of a general project aimed to photochemical studies of species with atmospheric interest, as for

* Corresponding author.
E-mail address: romano@quimica.unlp.edu.ar (R.M. Romano).

http://dx.doi.org/10.1016/j.jphotochem.2016.03.019
1010-6030/

example fluorinated alcohols (CF_3CH_2OH) [5], perfluorocarbons ($CF_3CF_2CF_2C(O)Cl$) [6], compounds containing the $-SO_2-$ group (FSO_2NCO [7], $ClSO_2NCO$) [8], among others. The main objective of these studies is the determination of the photochemical mechanisms through the detection of the photoproducts and reactive intermediates, allowing the modeling of possible atmospheric process. Light of different wavelength, ranging from visible to X ray radiation, as well as different detection techniques, are used in these investigations. Below the first ionization potential, in the region of visible and UV light, the fragmentation process occurring through free radicals and producing neutral species are followed mainly by IR spectroscopy [9,10]. When ionizing radiation is used, in the VUV and X ray region, electron and ionic species are detected [5–8].

In this work, electronic studies of pyrosulfuryl chloride were performed by a combination of photoelectron spectroscopy (PES) measurements using a He(I) lamp (to probe valence electrons) and electrons and ions detection after irradiation of the sample with tunable ionizing synchrotron light (for shallow and core electrons). The fragmentation mechanisms after single and double ionization processes were studied by means of coincidence techniques. The experimental results were interpreted with the assistance of density functional theory calculations. The photofragmentation mechanisms were modeled by the formalism proposed by Eland [11].

2. Material and methods

2.1. Sample preparation

$ClSO_2OSO_2Cl$ was obtained through the reaction of CCl_4 with SO_3, following a method slightly modified with respect to the one reported in Brauer [12]. In a Carius tube closed by a Young's valve, fresh prepared SO_3 (obtained by thermal decomposition of $K_2S_2O_7$) was condensed on CCl_4. After the reaction mixture had been stirred at approximately 80 °C for 5 h, the volatile components were fractionated under dynamic vacuum through traps held at −50, −80, −110, and −196 °C. $ClSO_2OSO_2Cl$ was collected in the −80 °C trap. The purity of the compounds was checked by means of the FTIR (vapour) and Raman (liquid) spectra.

2.2. Photoelectron spectroscopy

The photoelectron spectrum was recorded on a double-chamber UPS-II machine, which was designed specifically to detect transient species as described elsewhere [13,14], at a resolution of about 30 meV indicated by the standard $Ar^+(^2P_{3/2})$ photoelectron band. Ionization is provided by single-wavelength HeI radiation. Experimental vertical ionization energies were calibrated with methyl iodide.

2.3. Synchrotron experiments

The synchrotron radiation was used at the Laboratório Nacional de Luz Síncrotron (LNLS), Campinas, São Paulo, Brazil [15]. Linearly polarized light monochromatized by a toroidal grating monochromator (TGM beamline, from 12 to 310 eV) or a spherical grating monochromator (SGM beamline, from 200 to 1000 eV) [16] intersects the effusive gaseous sample inside a high-vacuum experimental station [17] at a base pressure in the range of 10^{-8} mbar. During the experiments, the pressure was maintained below 2×10^{-6} mbar. The resolution power is better than 400 in the TGM beam-line, reaching a $E/\Delta E = 550$ in the range from 10 to 21 eV. Energy calibration in the S 2p energy region was established by means of the S $2p \rightarrow 6a1g$ and S $2p \rightarrow 2t2g$ absorption resonances in SF_6 [18]. In the SGM beamline the resolution is $E/\Delta E = 1000$. The intensity of the beam was recorded by a light-sensitive diode. The ions produced by the interaction of the gaseous sample with the light beam were detected by means of a Time-Of-Flight (TOF) mass spectrometer of the Wiley-McLaren type for both PEPICO (Photoelectron-Photoion-Coincidence) and PEPIPICO (Photoelectron-Photoion-Photoion-Coincidence) measurements [19,20]. This instrument was constructed at the Institute of Physics, Brasilia University, Brasilia, Brazil [21]. The axis of the TOF spectrometer is perpendicular to the photon beam and parallel to the plane of the storage ring. Electrons are accelerated to a Multi Channel Plate (MCP) and recorded without energy analysis. This event starts the flight time determination process for the corresponding ion, which was consequently accelerated towards another MCP detector. High-purity vacuum-ultraviolet photons are used; the problem of contamination by high-order harmonics can be suppressed by the gas-phase harmonic filter installed at the TGM beam line at the LNLS [22–24].

2.4. Theoretical methods

OVGF (Outer Valence Green Function) and P3 (Partial Third Order) calculations using the 6-311+G(d) basis set at B3LYP/6-311+G(d)-optimized geometry of the most stable conformer have been performed on $ClSO_2OSO_2Cl$ in its ground electronic state using the Gaussian03 program package [25]. The energies of the possible fragments arising from the dissociation of the $ClSO_2OSO_2Cl^{\bullet+}$ parent low-lying radical ion were calculated at the UB3LYP/6-311+G(d) level of approximation.

3. Results and discussion

3.1. Photoelectron spectroscopy and photoionization mass spectroscopy

The valence electron properties of pyrosulfuryl chloride, $ClSO_2OSO_2Cl$, were investigated by means of photoelectron spectroscopy. The ionization energies of the outer valence electrons were determined, and the characters of the molecular orbitals involved were assigned according to the B3LYP calculations.

Fig. 1 shows the gas-phase photoelectron spectrum of $ClSO_2OSO_2Cl$ (in gray trace) taken with single-wavelength He(I)

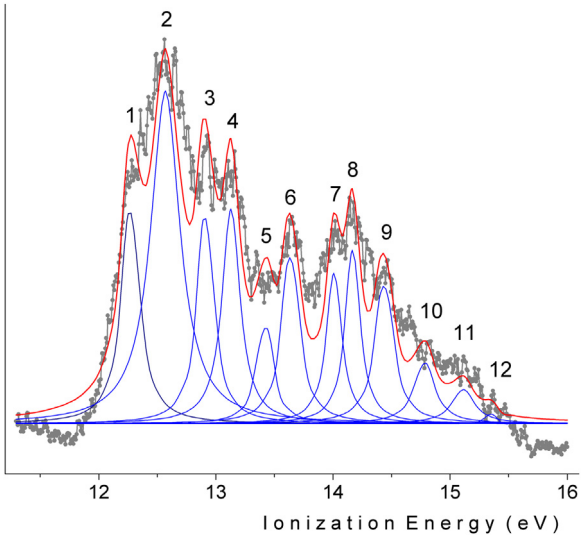

Fig. 1. He(I) photoelectron spectrum of $ClSO_2OSO_2Cl$. Experimental spectrum (grey trace), deconvoluted peaks (blue traces) and sum of the deconvoluted peaks (red trace). (For interpretation of the references to colour in this figure legend, the reader is referred to the web version of this article.)

radiation of 21.2 eV. As can be observed in the figure, the spectrum presents a complex structure with overlapped bands, due to the similar character of the ionized valence electrons. The spectrum was then deconvoluted, using lorentzian bands. The resulting individual peaks are presented in blue in Fig. 1 and the maxima of the bands are listed in Table 1. The first ionization potential was observed at 12.25 eV, in agreement with reported values for related molecules possessing the $-SO_2-$ group (SO_2, 12.50 eV [26]; SO_2Cl_2, 12.41 eV [27]; $ClSO_2N_3$, 11.43 eV [27]; $ClSO_2NCO$, 12.02 eV [27]; FSO_2NCO, 12.3 eV [7]).

The interpretation and assignment of the photoelectron spectrum was performed with the aid of different theoretical calculations, OVGF/6-311+G(d) and P3/6-311+G(d), which correlated well with the experimental values for compounds containing the $X-SO_2-$ group, with X = halogen [7]. The vertical ionization energies, as well as the approximate character of the molecular orbitals involved in each ionization, were calculated for the optimized most stable molecular structure. The values are included in Table 1. An schematic representation of HOMO to HOMO-11, calculated with the NBO formalism at the B3P86/6-311+G(d) level of approximation, is presented as Supplementary Information (Fig. S1).

The first eight bands are assigned to ionization processes of non-bonding electrons formally located at the oxygen atom of each of the S=O groups, nO (S=O). The last four bands, corresponding to HOMO-8 to HOMO-11, are assigned to non-bonding electrons located at each of the chlorine atoms. As can be observed in Table 1, there is a very good correlation between the experimental deconvoluted ionization potentials and the calculated vertical ionization energies.

The He-I photoionization mass spectrum (PIMS) of $ClSO_2OSO_2Cl$ was measured simultaneously with the photoelectron spectrum. Only two broad peaks were observed in the spectrum, at m/z 64 and 99, assigned to SO_2^+ and $ClSO_2^+$, respectively. As it will be presented in the next section, this result is coincident with the main fragments, together with the lack of the parent ion, which is observed when the sample is irradiated with synchrotron light at 21 eV.

3.2. Photoelectron-photoion-photoion coincidence spectroscopy

The unimolecular fragmentation mechanisms of $ClSO_2OSO_2Cl$ after single photoionization with light in the valence electronic region were investigated by means of PEPICO (Photoelectron-Photoion-Coincidence) spectra as a function of the monochromatic synchrotron radiation energy. Each peak in the PEPICO spectra represents one particular mechanism, being the intensity of the peak proportional to the occurring probability of the given mechanism.

Below 12 eV, no signs of the production of ions were observed in the PEPICO spectra, in accordance with the value of 12.25 eV determined for the first ionization potential of the molecule (Table 1). When the gaseous sample was irradiated with photons at 12 eV, just inside the tail of the first ionization band of the photoelectron spectrum (see Fig. 1), some ions were detected in coincidence with the ejected electrons, although the ionization yield was very low, as expected. The spectrum, depicted in Fig. 2, clearly shows two group of peaks, at 214/216/218 and 179/181 a.m.u./z, assigned to the isotopologic contribution of the parent ion, M^+, and $(M-Cl)^+$, respectively. Even at this low energy, the lowest possible to produce ionization, the fragment formed by the loose of a chlorine atom, in a process described by Eq. (1), is more abundant than the parent ion.

$$ClSO_2OSO_2Cl^{\bullet+} \rightarrow Cl^{\bullet} + \mathbf{ClSO_2OSO_2^+} \quad (1)$$

The selective breaking of the $Cl-SO_2$ bond after ionization in the valence energy region was previously observed as the main photofragmentation mechanism for the related $ClSO_2NCO$ molecule [8]. This mechanism is also in agreement with the results obtained for the calculation of the possible fragmentation channels of $ClSO_2OSO_2Cl^{\bullet+}$, considering the rupture of only one single chemical bond. According to the UB3LYP/6-311+G(d)

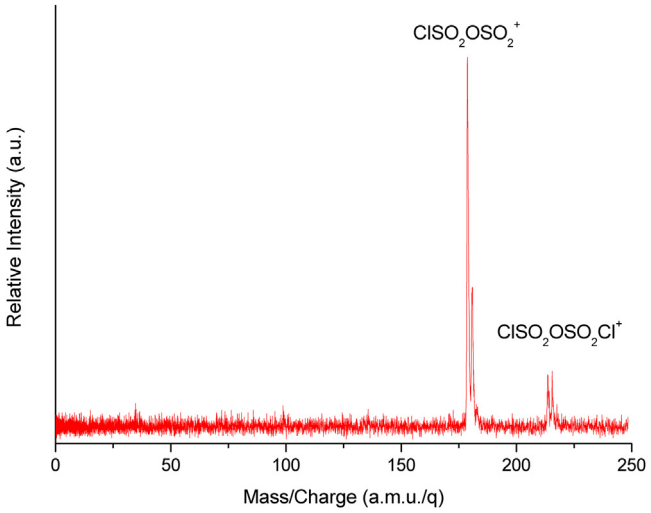

Fig. 2. PEPICO spectrum of $ClSO_2OSO_2Cl$ measured at 12 eV.

Table 1
Experimental ionization potentials (IP, eV), vertical ionization energies (Ev, eV) calculated with different theoretical approximations and tentative assignment to valence molecular orbitals of $ClSO_2OSO_2Cl$.

Peak	Exp.IP (eV)[a]	Ev (eV)		MO	Characeter
		OVGF/6-311+G(d)	P3/6-311+G(d)		
1	12.25	12.77	12.64	HOMO	nO (S=O)
2	12.57	12.85	12.71	HOMO – 1	nO (S=O)
3	12.89	13.03	13.05	HOMO – 2	nO (S=O)
4	13.12	13.16	13.19	HOMO – 3	nO (S=O)
5	13.44	13.72	13.48	HOMO – 4	nO (S=O)
6	13.61	13.83	13.46	HOMO – 5	nO (S=O)
7	14.00	14.18	13.74	HOMO – 6	nO (S=O)
8	14.16	14.42	14.15	HOMO – 7	nO (S=O)
9	14.40	14.72	14.27	HOMO – 8	nCl
10	14.80	14.86	14.41	HOMO – 9	nCl
11	15.12	15.09	14.63	HOMO – 10	nCl
12	15.36	15.78	15.24	HOMO – 11	nCl

[a] The experimental values correspond to the maxima of the deconvoluted peaks of Fig. 1.

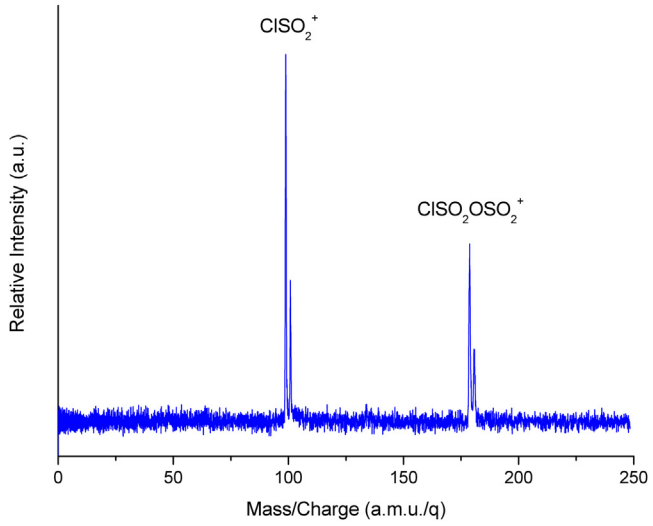

Fig. 3. PEPICO spectrum of $ClSO_2OSO_2Cl$ measured at 13 eV.

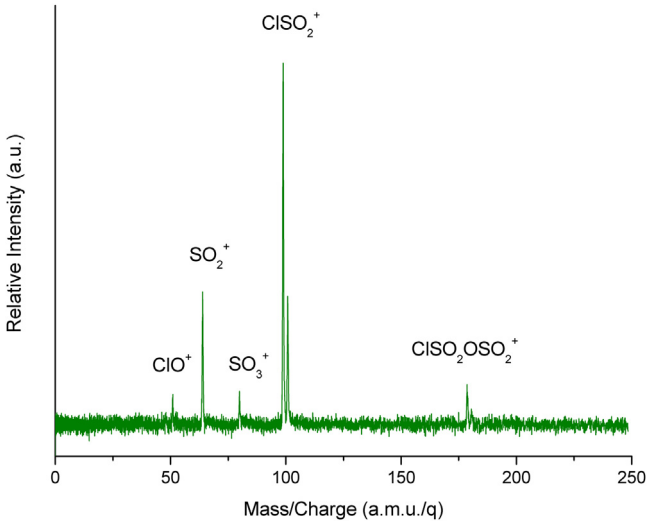

Fig. 4. PEPICO spectrum of $ClSO_2OSO_2Cl$ measured at 21 eV.

approximation, the products of Eq. (1), $ClSO_2OSO_2^+$ and $Cl^\bullet$, are 0.09 eV more stable than $M^{\bullet+}$. The breaking of the Cl–SO_2 bond to give Cl^+ and $ClSO_2OSO_2^\bullet$ is predicted, by the same theoretical approximation, 5.40 eV higher in energy than the first mechanism, in accordance with the expected behavior. On the other hand, the fragmentation of the parent ion through one of the S–O single bonds can produce either $ClSO_2O^\bullet$ and $ClSO_2^+$ or $ClSO_2^\bullet$ and $ClSO_2O^+$ fragments. According to the UB3LYP/6-311+G(d) approximation, formation of the first two products are predicted 0.40 eV higher in energy than $M^{\bullet+}$, while in the second mechanism the fragments were found to be 2.32 eV less stable than the parent ion.

In the spectrum taken with synchrotron light of 13 eV, depicted in Fig. 3, the molecular ion was no longer detected. Besides the $ClSO_2OSO_2^+$ fragment, a group of peaks at 99/101 a.m.u./z, assigned to $ClSO_2^+$, were observed. The presence of this positive ion can arise either from direct fragmentation of $M^{\bullet+}$ through the rupture of one of the S–O single bond (Eq. (2)), or from $ClSO_2OSO_2^+$, as schematized in Eq. (3). The energy difference between the products and $M^{\bullet+}$ is similar for both mechanisms: 0.40 eV for the channel schematized by Eq. (2) and 0.56 eV for the mechanism described by Eqs. (1) and (3).

$$ClSO_2OSO_2Cl^{\bullet+} \rightarrow ClSO_2O^\bullet + \mathbf{ClSO_2^+} \quad (2)$$

$$ClSO_2OSO_2^+ \rightarrow SO_3 + \mathbf{ClSO_2^+} \quad (3)$$

Although $ClSO_2^+$ and $ClSO_2OSO_2^+$ are observed at all energies studied between 12 and 21 eV (the use of a Ne filter to cut the high-order harmonics precludes the irradiation of the sample with synchrotron radiation above 21 eV), new fragmentation channels are opened as the energy of the light increases. From 18 eV, SO_2^+ and also ClO^+, originated in an atomic rearrangement, appear in the PEPICO spectra, and their relative intensities continuously grow with the excitation energy.

One more fragmentation channel in this energy region is observed from 19 eV, with the detection of SO_3^+. Fig. 4 shows the PEPICO spectra taken at 21 eV, and Fig. 5 presents the plot of the relative intensity of the different fragments as a function of the incident synchrotron light. In agreement with the predicted energy profile of the possible photoproducts, Cl^+ and $ClSO_2O^+$ fragments were not detected in the PEPICO spectra taken at any of the irradiation energy used in the valence electronic region.

Not only single but also double and, in less extent, multiple ionization processes are feasible when the gaseous sample is excited with photons in the energy range of inner-electrons. In the event of double ionization, the M^{2+} parent ion usually produces two single charged species and, possibly, neutral fragments. PEPIPICO (Photoelectron-Photoion-Photoion-Coincidence) spectroscopy allows the correlation of two single-charged ions proceeding from M^{2+}, observed as islands in a bidimensional spectrum, and thus the study of fragmentation mechanisms. In the next paragraphs we present the previous determination of the energies of the inner electrons of the molecule that will be subsequently selected for the study of the photofragmentation mechanisms, in order to investigate the presence of site-specific processes.

Fig. 6 depicts the Total Ion Yield (TIY) spectra, without discrimination of the ion masses, as a function of the energy of the incident light, in four selected energy regions, corresponding to the ionization of S 2p, Cl 2p, S 2s and O 1s electrons. The ionization threshold of 2p electrons of the S atoms is located at approximately 182.4 eV. At least six peaks are observed at lower energies, at 168.4,

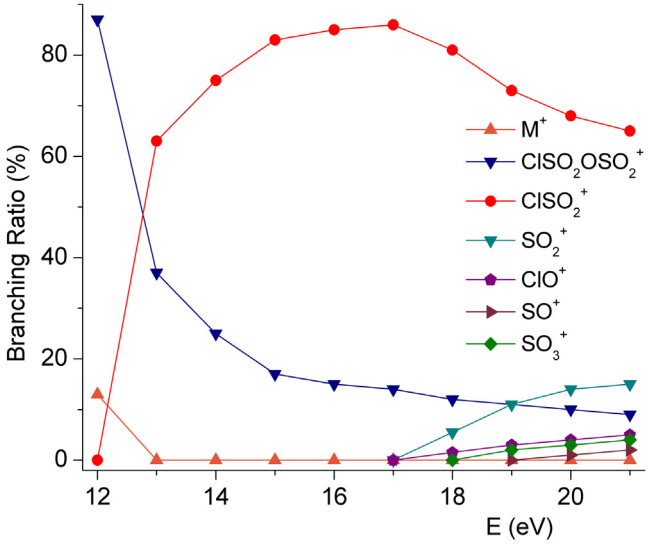

Fig. 5. Branching ratios of selected ions in the PEPICO spectra of $ClSO_2OSO_2Cl$ as a function of the energy of the incident synchrotron radiation.

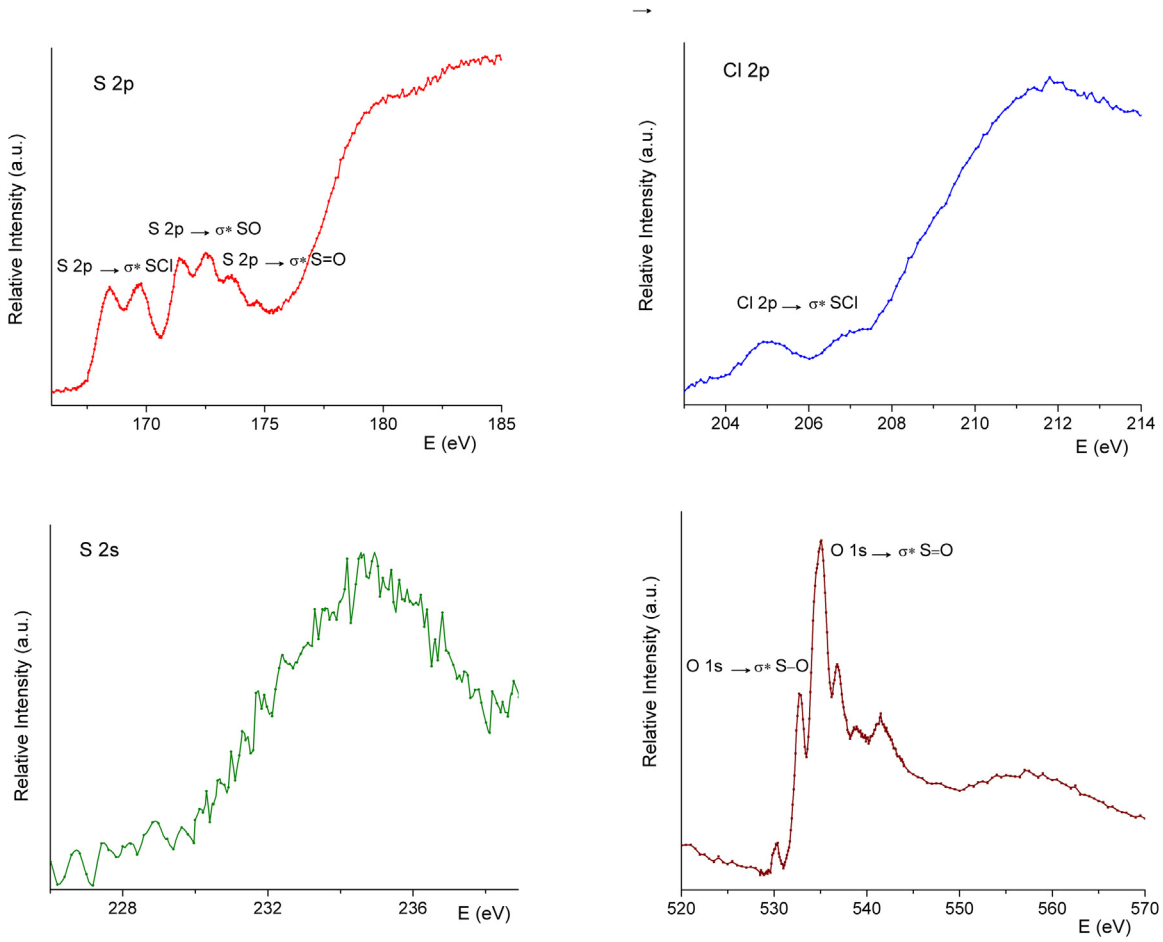

Fig. 6. Total Ion Yield spectra of $ClSO_2OSO_2Cl$ taken in the S 2p, Cl 2p, S 2s and O 1s energy regions.

169.8, 171.4, 172.3, 173.7 and 174.7 eV. According with the predicted order and character of the LUMO's of $ClSO_2OSO_2Cl$, schematized in Fig. S2 of the Supplementary information, these peaks can be tentatively assigned to S 2p → LUMO/LUMO + 1 (σ^*S–Cl), S 2p → LUMO + 2/ + 3 (σ^*S–O) and S 2p → LUMO + 4 to LUMO + 7 σ^*(S=O) resonant transitions. The $2p_{3/2}$ and $2p_{1/2}$ splitting of each transition, expected with an energy difference of about 1.2 eV and an intensity ratio 2:1 [28], may be overlapped with the bands.

Low-intensity signals at 205.0 and 206.5 eV observed in Fig. 6 were interpreted as resonant transitions of Cl 2p electrons to LUMO and LUMO + 1, with σ^* S–Cl character. These transitions were also proposed in the interpretation of the spectra of the following related molecules: SCl_2, S_2Cl_2, $SOCl_2$ and SO_2Cl_2 [29]. The ionization threshold of the Cl 2p electrons occurs close to 211.5 eV. The ionization energy of S 2s electrons is located at 234.9 eV (see Fig. 6), in agreement with the observed for related molecules [7,8].

In the O 1s region the spectrum is composed by a complex pattern, with overlapped bands at 530.2, 532.8, 535.0, 536.9, 538.8 and 541.5 eV, probably originated in O 1s → σ^* (S–O) and O 1s → σ^* (S=O) resonant transitions from the different oxygen atoms. The ionization O 1s threshold is observed at approximately 557.3 eV.

The bidimensional PEPIPICO spectra excited with synchrotron light of different energies, coincident with the resonances and ionization thresholds described in the precedent paragraphs, were measured. From the shape and slope of the coincidence islands in the PEPIPICO spectra, and by the comparison with the predictions of simple models based in the momentum conservation during the fragmentation, the photofragmentation mechanisms can be inferred. From a detailed inspection of the spectra we can conclude that the fragmentation channels leading to the formation of a pair of single-charged species are independent of the incident energy, although the relative intensity of each of them slightly depends on the energy of the excited light.

The most intense island at all the investigated energies is composed by the O^+/S^+ pair (~37% at 535 eV), followed by the O^+/Cl^+ pair (~22% at 535 eV). The coincidence islands formed by non-atomic fragments have lower intensities than the atomic ones. Fragmentation mechanisms leading to SO^+ fragment are most probable than channels that generate other non-atomic species. In all cases the islands present a parallelogram shape.

Table 2 compiles some of the mechanisms proposed to explain the coincidence islands observed in the PEPIPICO spectra. In the first column of Table the initial step (or steps) of each mechanism is presented, while the final steps are represented in the second column. This division was made only because some of the dissociation mechanisms start with the same fragmentation channel. The Table also includes the observed ions (the neutral fragments are not detected with this technique), the theoretical slope calculated with the formalisms proposed by Eland [11], the experimental slope measured from the bidimensional spectra, and the denomination of the mechanisms. In the Eland's formalisms, the requirement of the linear momentum conservation of the fragments allows the deduction of the theoretical slope of the coincidence islands, according with different proposed mechanisms. In the case of two-body dissociation, the coincidence island in the PEPIPICO spectra presents a "cigar" shape with slope of −1. In

Table 2
Photofragmentation mechanisms of $ClSO_2OSO_2Cl$.

Dissociation Pathways		Ions detected in coincidence	α_{calc}[a]	α_{exp}[b]	Mechanism[c]
Initial Steps	Final Steps				
$M^{2+} \rightarrow Cl^{\bullet} + ClSO_2OSO_2^{\bullet}2+$	$ClSO_2OSO_2^{\bullet}2+ \rightarrow SO_2^{\bullet}+ + ClSO_2O^+$ $SO_2^{\bullet}+ \rightarrow SO + \mathbf{O^{\bullet}}+$ $ClSO_2O^+ \rightarrow SO_3 + \mathbf{Cl^+}$	$\mathbf{O^+/Cl^+}$	−1.2	−1.2	CSD
	$ClSO_2OSO_2^{\bullet}2+ \rightarrow SO_2^{\bullet}+ + ClSO_2O^+$ $SO_2^{\bullet}+ \rightarrow O_2 + \mathbf{S^{\bullet}}+$ $ClSO_2O^+ \rightarrow O_3 + \mathbf{ClS^+}$	$\mathbf{S^+/ClS^+}$	−1.2	−1.2	CSD
	$ClSO_2OSO_2^{\bullet}2+ \rightarrow Cl^{\bullet} + SO_2OSO_2^{2+}$ $SO_2OSO_2^{2+} \rightarrow SO_2^{\bullet}+ + SO_3^{\bullet}+$ $SO_2^{\bullet}+ \rightarrow O_2 + \mathbf{S^{\bullet}}+$ $SO_3^{\bullet}+ \rightarrow O_2 + \mathbf{SO^{\bullet}}+$	$\mathbf{S^+/SO^+}$	−1.2	−1.2	CSD
$M^{2+} \rightarrow ClSO_2O^{\bullet} + ClSO_2^{\bullet}2+$	$ClSO_2^{\bullet}2+ \rightarrow \mathbf{Cl^+} + \mathbf{SO_2^{\bullet}}+$	$\mathbf{Cl^+/SO_2^+}$	−1.0	−1.0	DCS
	$ClSO_2^{\bullet}2+ \rightarrow O + ClSO^{\bullet}2+$ $ClSO^{\bullet}2+ \rightarrow \mathbf{Cl^+} + \mathbf{SO^{\bullet}}+$	$\mathbf{Cl^+/SO^+}$	−1.0	−1.0	DCS
	$ClSO_2^{\bullet}2+ \rightarrow \mathbf{Cl^+} + SO_2^{\bullet}+$ $SO_2^{\bullet}+ \rightarrow O_2 + \mathbf{S^{\bullet}}+$	$\mathbf{Cl^+/S^+}$	−2.0	−1.9	SD-DCS
	$ClSO_2^{\bullet}2+ \rightarrow \mathbf{O^{\bullet}}+ + ClSO^+$ $ClSO^+ \rightarrow O + \mathbf{ClS^+}$	$\mathbf{O^+/ClS^+}$	−0.8	−0.8	SD-DCS
	$ClSO_2^{\bullet}2+ \rightarrow Cl^{\bullet} + SO_2^{2+}$ $SO_2^{2+} \rightarrow \mathbf{O^{\bullet}}+ + \mathbf{SO^{\bullet}}+$	$\mathbf{O^+/SO^+}$	−1.0	−1.0	DCS
$M^{2+} \rightarrow ClSO_2O^+ + ClSO_2^+$	$ClSO_2^+ \rightarrow \mathbf{Cl^+} + SO_2$ $ClSO_2O^+ \rightarrow \mathbf{Cl^+} + SO_3$	$\mathbf{Cl^+/Cl^+}$	−1.2	−1.2	CSD
$M^{2+} \rightarrow ClSO_2^{\bullet} + ClSO_2O^{\bullet}2+$	$ClSO_2O^{\bullet}2+ \rightarrow \mathbf{O^{\bullet}}+ + ClSO_2^+$ $ClSO_2^+ \rightarrow Cl^{\bullet} + \mathbf{SO_2^{\bullet}}+$	$\mathbf{O^+/SO_2^+}$	-0.6_5	-0.6_5	SD-DCS
	$ClSO_2O^{\bullet}2+ \rightarrow \mathbf{O^{\bullet}}+ + ClSO_2^+$ $ClSO_2^+ \rightarrow Cl^{\bullet} + SO_2^{\bullet}+$ $SO_2^{\bullet}+ \rightarrow O_2 + \mathbf{S^{\bullet}}+$	$\mathbf{O^+/S^+}$	−0.5	−0.5	SD-DCS

[a] Theoretical slope of the coincidence island calculated with the formalisms proposed by Eland [11].
[b] Experimental slope of the coincidence island measured from the bidimensional PEPIPICO spectra.
[c] CSD: Competitive Secondary Decay; DCS: Deferred Charge Separation; SD-DCS: Secondary Decay after a Deferred Charge Separation.

a three-body fragmentation of a doubly charged molecule, the possible mechanisms are identified as Deferred Charge Separation (DCS), Secondary Decay (SD), and Concerted Dissociation (CD). Two additional mechanisms were proposed for four-body decay [30]: Secondary Decay after a Deferred Charge Separation (SD-DCS) and Competitive Secondary Decay (CSD).

All mechanisms proposed in Table 2 start with the rupture of one bond of M^{2+}, either the Cl–S or the O–S single bond. The fragmentation through the Cl–S bond produces a chlorine radical and a $ClSO_2OSO_2^{2+}$ fragment. In two of the mechanisms, this species subsequently dissociate into $ClSO_2O^+$ and SO_2^+ ions, followed by competitive secondary decays, ended either in O^+/Cl^+ or S^+/ClS^+ pair of ions. In a third mechanism, $ClSO_2OSO_2^{2+}$ loses the remaining chlorine atom, and then the formed $SO_2OSO_2^{2+}$ species dissociates through the O–S single bond to produce SO_2^+ and SO_3^+, that conduct to S^+ and SO^+ ions in a competitive secondary decay pathway. An initial step involving the simultaneous loss of both Cl radicals with the formation of molecular chlorine cannot be discarded to explain the experimental slope of the S^+/SO^+ coincidence island in the PEPIPICO spectra. Since neutral fragments are not detected with the experimental setup used in the experiments, these two possibilities cannot be discerned.

After the rupture of the O–S single bond of M^{2+}, the double charge can be retained by only one fragment, either $ClSO_2O^{2+}$ or $ClSO_2^{2+}$, or distributed between the two species, originating $ClISO_2O^+$ and $ClSO_2^+$ single-charged fragments. These mechanisms conduct to the coincidence island involving Cl^+, with Cl^+, S^+, SO^+ and SO_2^+, and O^+, with S^+, SO^+, ClS^+ and SO_2^+.

Besides the coincidence presented in Table 2, the O^+/O^+, S^+/S^+, S^+/SO_2^+, SO^+/SO^+, SO^+/SO_2^+, and SO_2^+/SO_2^+ pairs were also detected in coincidence. A plausible interpretation of the −1.0 experimental slope of these islands is that the species were produced thorough concerted mechanisms. Fig. 7 shows the PEPIPICO spectrum taken at 535 eV, the energy determined for the resonance of a O 1s → σ* (S=O) transition according to Fig. 6, and the contour maps of two selected coincidence island, Cl^+/SO^+ (with $\alpha_{exp} = -1.0$) and O^+/S^+ (with $\alpha_{exp} = -0.5$).

4. Conclusions

The electronic properties of $ClSO_2OSO_2Cl$ were determined by a combination of He(I) photoelectron spectroscopy and Total Ion

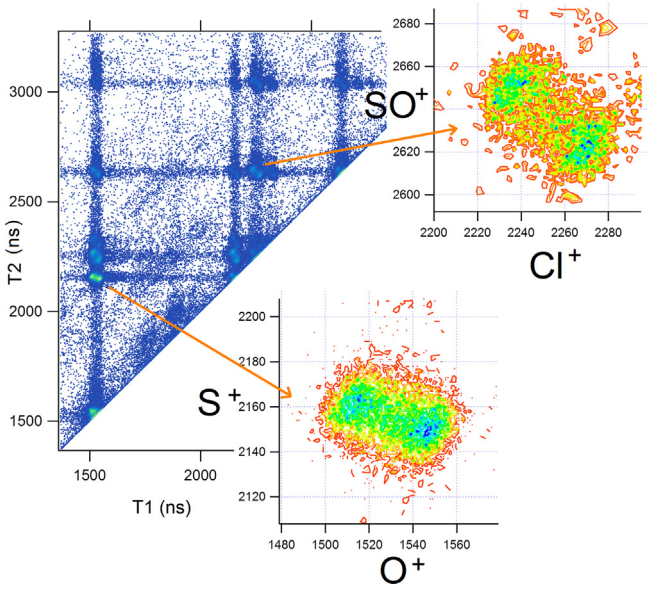

Fig. 7. PEPIPICO spectrum of $ClSO_2OSO_2Cl$ taken at 535 eV (left) and contour plots of selected coincidence islands: Cl^+/SO^+ (top-right) and O^+/S^+ (bottom-right).

Yield spectroscopy using synchrotron radiation. The first ionization potential was found at 12.25 eV, and the PES spectrum was interpreted in terms of twelve ionizations of oxygen and chlorine non-bonding electrons. Indirect information about the character and energy differences of the LUMOs could be accessed from the TIY spectra taken in resonance with shallow and core electrons. According to theoretical predictions, LUMO and LUMO+1 of $ClSO_2OSO_2Cl$ can be both approximately described as σ^*S-Cl. The experimental energy difference between these two orbitals was found to be 1.4 eV (from the S 2p → LUMO/LUMO+1 (σ^*S-Cl) transitions in the S 2p TIY spectrum) and 1.5 eV (from the Cl 2p → LUMO/LUMO+1 (σ^*S-Cl) transitions in the Cl 2p TIY spectrum), corroborating the proposed assignment.

Photofragmentation mechanisms of $ClSO_2OSO_2Cl$ following single and double ionization were studied by means of PEPICO and PEPIPICO coincidence spectroscopies, respectively. At low energies, the main fragmentation mechanism leads to the loss of a chlorine radical and the concomitant formation of $ClSO_2OSO_2^+$ fragment. As the irradiation energy increases, new ionic fragments were detected, arising either by new fragmentation channels opened for the parent ion, or by a subsequent fragmentation of $ClSO_2OSO_2^+$. Considering the last possibility, the following mechanisms can be suggested:

$$M + h\nu \rightarrow M^{\bullet+} + e^-$$

$$M^{\bullet+} \rightarrow Cl^{\bullet} + ClSO_2OSO_2^+ \qquad 12.0 < h\nu < 13.8 \text{ eV}$$

$$ClSO_2OSO_2^+ \rightarrow ClSO_2^+ + SO_3 \qquad 13.8 < h\nu < 21.5 \text{ eV}$$

$$CLSO_2^+ \rightarrow SO_2^{\bullet+} + Cl^{\bullet} \qquad 18.0 < h\nu < 21.5 \text{ eV}$$

The fragmentation mechanisms were proposed by the comparison of the experimental slopes of the coincidence islands in the PEPIPICO spectra with the theoretical slopes calculated by the Eland's formalism. M^{2+} species evolves following several different channels, all of them started from the rupture of either Cl−S or O−S single bonds. The fragmentation channels of pyrosulfuryl chloride after double ionization were found to be independent of the incident radiation energy, denoting the absence of significant site-specific processes.

Acknowledgments

This work has been largely supported by the Brazilian Synchrotron Light Source (LNLS) under Proposals TGM-10926 and SGM-11670. The authors wish to thank Arnaldo Naves de Brito and his research group for fruitful discussions and generous collaboration during their several stays in Campinas and the TGM and SGM beamline staffs for their assistance throughout the experiments. They are also indebted to the Agencia Nacional de Promoción Científica y Tecnológica (ANPCyT),Consejo Nacional de Investigaciones Científicas y Técnicas (CONICET), and the Facultad de Ciencias Exactas, Universidad Nacional de La Plata for financial support.

Appendix A. Supplementary data

Supplementary data associated with this article can be found, in the online version, at http://dx.doi.org/10.1016/j.jphotochem.2016.03.019.

References

[1] R.M. Romano, C.O. Della Védova, H. Beckers, H. Willner, Photochemistry of $SO_2/Cl_2/O_2$ gas mixtures: synthesis of the new peroxide $ClSO_2OOSO_2Cl$, Inorg. Chem. 48 (2009) 1906–1910.
[2] W.B. Demore, M.-T. Leu, R.H. Smith, Y.L. Yung, Laboratory studies on the reactions between chlorine, sulfur dioxide, and oxygen: implications for the venus stratosphere, Icarus 63 (1985) 347–353.
[3] W. Prandtl, P. Borinski, Über das pyrosulfurylchloride $S_2O_5Cl_2$, Z. Anorg. Chem. 62 (1909) 24–33.
[4] C.R. Sanger, E.R. Riegel, Pyrosulfurylchlorid und chlorsulfonsäure, Z. Anorg. Chem. 76 (1912) 79–128.
[5] Y.B. Bava, Y. Berrueta Martínez, A. Moreno Betancourt, M.F. Erben, R.L. Cavasso Filho, C.O. Della Védova, R.M. Romano, Ionic fragmentation mechanisms of 2,2,2-trifluoroethanol following excitation with synchrotron radiation, ChemPhysChem 16 (2015) 322–330.
[6] Y. Berrueta Martínez, Y.B. Bava, M.F. Erben, R.L. Cavasso Filho, R.M. Romano, C. O. Della Védova, Photoexcitation photoionization, and photofragmentantion of $CF_3CF_2CF_2C(O)Cl$ using synchrotron radiation between 13 and 720, J. Phys. Chem. A 119 (2015) 1894–1905.
[7] A. Moreno Betancourt, A. Flores Antognini, M.F. Erben, R.L. Cavasso Filho, S. Tong, M. Ge, C.O. Della Védova, R.M. Romano, Electronic properties of fluorosulfonyl isocyanate, FSO_2NCO: a photoelectron spectroscopy and synchrotron photoionization study, J. Phys. Chem. A 117 (2013) 9179–9188.
[8] A. Moreno Betancourt, Y.B. Bava, Y. Berrueta Martínez, M.F. Erben, R.L. Cavasso Filho, C.O. Della Védova, R.M. Romano, Photofragmentation mechanisms of chlorosulfonyl isocyanate, $ClSO_2NCO$ excited with synchrotron radiation between 12 and 550 eV, J. Phys. Chem. A 119 (2015) 8021–8030.
[9] N.L. Robles, A. Flores Antognini, R.M. Romano, Formation of XNCO species (X = F, Cl) through matrix-isolation photochemistry of XSO_2NCO molecules, J. Photochem. Photobiol. A Chem. 223 (2011) 194–201.
[10] R.M. Romano, C.O. Della Védova, A.J. Downs, Methanesulfenyl fluoride, CH_3SF, a missing link in the family of sulfenyl halides: formation and characterization through the matrix photochemistry of methyl thiofluoroformate $FC(O)SCH_3$, Chem. Eur. J. 13 (2007) 8185–8192.
[11] J.H.D. Eland, The dynamics of three-Body dissociations of dications studied by the triple coincidence technique PEPIPICO, Mol. Phys. 61 (1987) 725–745.
[12] G. Brauer, Handbuch Der Präparativen Anorganischen Chemie, Ferdinand Enke Stuttgart, 1975.
[13] L. Yao, M. Ge, W. Wang, X. Zeng, Z. Sun, D. Wang, Gas-Phase generation and electronic structure investigation of chlorosulfanyl thiocyanate, ClSSCN, Inorg. Chem. 45 (2006) 5971–5975.
[14] L. Du, L. Yao, X. Zeng, M. Ge, D. Wang, HeI photoelectron spectroscopy and theoretical study of trichloromethanesulfenyl acetate $CCl_3SOC(O)CH_3$, and trichloromethanesulfenyl trifluoroacetate, $CCl_3SOC(O)CF_3$, J. Phys. Chem. A 111 (2007) 4944–4949.
[15] A.R.D. Lira, A. Rodrigues, C. Gonçalves da Silva, C. Pardine, D. Scorzato, F. Wisnivesky, G.S. Rafael, G. Franco, L. Lin, et al., First Year Operation of the Brazilian Sinchrotron Light Source, European Particle Accelerator Conference, Stockholm, 1998.
[16] P. de, T. Fonseca, J.G. Pacheco, E. Samogin, A.R.B. de Castro, Vacuum ultraviolet beam lines at laboratório nacional de luz Síncrotron, the brazilian synchrotron source, Rev. Sci. Instrum. 63 (1992) 1256–1259.
[17] F. Burmeister, L.H. Coutinho, R.R.T. Marinho, M.G.P. Homem, M.A.A. de Morais, A. Mocellin, O. Björneholm, S.L. Sorensen, P. de, T. Fonseca, A. Lindgren, et al., Description and performance of an electron-ion coincidence TOF spectrometer used at the brazilian synchrotron facility LNLS, J. Electron Spectrosc. Relat. Phenom. 180 (2010) 6–13.
[18] A. Kivimaki, J. Alvarez Ruiz, P. Erman, P. Hatherly, E. Melero García, E. Rachlew, J. Rius i Riu, M. Stankiewicz, An energy resolved electron–ion coincidence study near the S 2p thresholds of the SF_6 molecule, J. Phys. B 36 (2003) 781–791.
[19] L.J. Frasinski, M. Stankiewicz, K.J. Randall, P.A. Hatherly, Dissociative photoionisation of molecules probed by triple coincidence; double time-of-flight techniques, J. Phys. B 19 (1986) L819–L824.
[20] J.H.D. Eland, F.S. Wort, R.N.A. Royds, Photoelectron-ion–ion triple coincidence technique for the study of double photoionization and its consequences, J. Electron Spectrosc. Relat. Phenom. 41 (1986) 297–309.
[21] A. Naves de Brito, R. Feifel, A. Mocellin, A.B. Machado, S. Sundin, I. Hjelte, S.L. Sorensen, O. Björneholm, Femtosecond dissociation dynamics of core excited molecular water, Chem. Phys. Lett. 309 (1999) 377–385.
[22] R.L. Cavasso Filho, M.G.P. Homem, R. Landers, A. Naves de Brito, Advances on the brazilian toroidal grating monochromator (TGM) beamline, J. Electron Spectrosc. Relat. Phenom. 144–147 (2005) 1125–1127.
[23] R.L. Cavasso Filho, A.F. Lago, M.G.P. Homem, S. Pilling, A. Naves de Brito, Delivering high-purity vacuum ultraviolet photons at the brazilian toroidal grating monochromator (TGM) beamline, J. Electron Spectrosc. Relat. Phenom. 156–158 (2007) 168–171.
[24] R.L. Cavasso Filho, M.G.P. Homem, P. de, T. Fonseca, A. Naves de Brito, A synchrotron beamline for delivering high purity vacuum ultraviolet photons, Rev. Sci. Instr. 78 (2007) 115104.
[25] M.J. Frisch, G.W. Trucks, H.B. Schlegel, et al., Gaussian 03, Revision C.02, Gaussian Inc., Wallingford CT, 2004.

[26] D. Chadwick, D.C. Frost, F.G. Herring, A. Katrib, C.A. McDowell, R.A.N. McLean, Photoelectron spectra of sulfuryl and thionyl halides, Can. J. Chem. 51 (1973) 1893–1905.
[27] F. Liu, X. Zeng, W. Wang, L. Meng, S. Zheng, M. Ge, D. Wang, Photoelectron spectra and electronic structures of some chlorosulfonyl pseudohalides, Spectrochim. Acta Part A 63 (2006) 111–116.
[28] G. Cooper, E.B. Zarate, R.K. Jones, C.E. Brion, Absolute oscillator strengths for photoabsorption, photoionization and ionic photofragmentation of sulphur dioxide. II. The S 2p and 2s inner shells, Chem. Phys. 150 (1991) 251–261.
[29] A.P. Hitchcock, S. Bodeur, M. Tronc, Sulfur and chlorine K-shell X-ray absorption spectra of SCl_2, S_2Cl_2 $SOCl_2$, and SO_2Cl_2, Chem. Phys. 115 (1987) 93–101.
[30] M. Simon, T. Lebrun, R. Martins, G.G.B. de Souza, I. Nenner, M. Lavollee, P. Morin, Multicoincidence mass spectrometry applied to hexamethyldisilane excited around the silicon 2p edge, J. Phys. Chem. 97 (1987) 5528–5537.